# Finite Element Modeling of Flow Through Ceramic Pot Filters

By
Anna C. Kelly
B.S. Environmental Engineering Science
Massachusetts Institute of Technology, 2012

Submitted to the Department of Civil and Environmental Engineering in
Partial Fulfillment of the Requirements of the Degree of

Master of Engineering
In Civil and Environmental Engineering
at the

MASSACHUSETTS INSTITUTE OF TECHNOLOGY

June 2013





Signature of Author _____
Anna C. Kelly
Department of Civil and Environmental Engineering
May 10, 2013

Certified by _____
Peter Shanahan
Senior Lecturer of Civil and Environmental Engineering
Thesis Supervisor

Accepted by _____
Heidi M. Nepf
Chair, Departmental Committee for Graduate Students

# Finite Element Modeling of Flow Through Ceramic Pot Filters

by
Anna C. Kelly

Submitted to the Department of Civil and Environmental Engineering on May 10, 2013, in Partial Fulfillment of the Requirements for the Degree of Master of Engineering in Civil and Environmental Engineering

**Abstract**

Pure Home Water (PHW) is an organization based in Tamale, Ghana that manufactures and distributes ceramic water filters. While many ceramic filter factories manufacture flowerpot-shaped filters, PHW has transitioned from the flowerpot shape, to a paraboloid shape, and finally to a hemispheric filter shape. The PHW factory conducts flow-rate testing as part of their quality control process and has documented a wide range of flow rates for the hemispheric filter as compared to the global standard. This thesis uses finite-element groundwater-flow modeling software to develop models of flow through three different ceramic filter shapes: flowerpot, paraboloid, and hemispheric filters. A sensitivity analysis was then conducted for each filter shape by simulating flow through the filter for a range of hydraulic conductivities. It was found that the hemispheric filter shape produces a higher flow rate than the flowerpot filter for a given hydraulic conductivity, and that the flow rate through the hemispheric filter is more sensitive to changes in hydraulic conductivity.

Thesis Supervisor: Peter Shanahan
Title: Senior Lecturer of Civil and Environmental Engineering

**Acknowledgements**
I would like to thank the following people for their invaluable assistance in finishing this thesis:

Pete Shanahan, for taking me on as an advisee with incredible good humor and providing constant and much-needed advice and encouragement.

Susan Murcott, for all of her hard work and for providing the initial inspiration for this thesis.

Dr. Eric Adams, for his guidance in helping me to reorient my thesis when initial plans fell through.

The 2013 Ghana M.Eng team. It was incredible and inspiring to work with you all this year.

My fellow M.Eng-ers: y'all are awesome. I am constantly amazed by all of your talent and accomplishments, and I am so proud and grateful to be in your company. I could not imagine a better group of people to have spent this year with.

Mom, Dad, and Mame, for all of your love and support. You guys rock. Thank you.

## Table of Contents

# List of Tables

# List of Figures

# 1. Introduction

An estimated 778 million people in the world do not have access to improved drinking water (WHO/UNICEF 2012). While this number represents an improvement on the 2004 estimate of 1.1 billion people, it also signifies a continuing need for water treatment solutions in the countries most affected by this problem. Diarrhea brought on by drinking contaminated water accounts for 1.87 million (19%) of childhood deaths each year (Boschi-Pinto et al, 2008).

## 1.1 Background

A number of non-governmental organizations (NGOs) have worked for years to develop and refine a ceramic water filter for point-of-use water treatment in developing countries. Most notably, Potters for Peace (PFP) have promoted ceramic filter manufacturing in over 20 countries (CMWG 2011), including in Ghana at the Pure Home Water (PHW) factory.

The goal underlying the manufacturing of ceramic pot filters is to create a self-sustaining business which produces filters using local materials and provides employment for local residents. The ceramic filters themselves are manufactured by mixing local clay with a combustible material, either sawdust or rice husk, adding water to achieve the correct consistency, and forming the filter shape using a press mold. The filters are then fired in a kiln, cooled, and saturated with water before undergoing flow rate testing. Once this testing is complete, the filters are allowed to dry again before a coating of colloidal silver is applied in order to aid bacteriological removal.

The finished ceramic filter is then placed inside of a food-grade plastic receptacle for in-home use. The hemispheric filter and its container are pictured in Figure 1-1. The upper "lip" of the filter sits on the edge of the plastic container, and water is poured into the filter from above. A removable plastic lid prevents exposure of the water inside the filter to outside elements. Water seeps through the filter and drains into the plastic container, creating a reservoir which can then be accessed using the spigot at the bottom of the container.

**Figure 1-1: Hemispheric ceramic filter element (left) and complete unit (right)**

The ceramic filters produced at PHW have evolved over the years from a flower-pot shape, to a paraboloid, to the current hemispheric filter design. As the filter design changes, quality control measures must be re-assessed.

## 1.2 Filter Effectiveness

The efficacy of a ceramic filter is evaluated by its ability to reduce bacterial contamination and turbidity of influent water. The reduction in bacteria is reported as percent reduction or log reduction value (LRV) (The Ceramics Manufacturing Working Group, 2011). Table 1-1, taken from the CDC's Best Practice Recommendations (The Ceramics Manufacturing Working Group, 2011), shows the relationship between LRV and percent reduction in bacterial contamination. The World Health Organization (WHO) has also developed a risk level classification system for water quality (WHO, 1997); to be compliant with WHO guidelines, water must contain fewer than 1 fecal coliform (*E. coli*) per 100 mL water sample.

**Table 1-1: Correspondence between LRV (standard reporting unit for bacteria removal) and percent reduction in bacterial contamination.**

| LRV | Reduction |
|---|---|
| 0.5 | 68% |
| 1 | 90% |
| 2 | 99% |
| 3 | 99.9% |

## 1.3 Production Variables and Quality Control Measures

The flow rate of a filter is a crucial quality control measure that can provide information about the efficacy of the filter in removing bacteria and reducing turbidity. Flow rate can also be indicative of production consistency; any defects or inconsistencies (cracks, holes, large pores) will result in a more widely variable flow rate for a given batch (The Ceramics Manufacturing Working Group, 2011). In the standard quality control process as described in the CDC's Best Practice Recommendations, flow rate is calculated for a full and completely saturated filter.

Acceptable flow rate values must be greater than 1 liter per hour in order to fulfill a family's daily needs, but must be low enough that the water passing through has sufficient contact time with the colloidal silver coating the filter in order to maximize pathogen removal (The Ceramics Manufacturing Working Group, 2011). The CDC Best Practice Recommendations suggest that the maximum flow rate should be 0.35 liters per hour per liter capacity of filter element; however, other research suggests that maximum acceptable flow rates may vary more widely than this.

Lantagne et al (2010) describe filter manufacturing processes in several developing countries: a factory in Nicaragua accepts filters with flow rates between 1 and 2 liters per hour, while the Aqua Pure factory in the Dominican Republic does not conduct flow rate testing due to its highly standardized manufacturing process. However, tests of the Aqua Pure filters showed them to operate below 1 liter per hour on average, consistently achieving 99% bacteria removal for flow rates below 1.7 liters per hour. Another study conducted in Nicaragua (Lantagne, 2001) revealed acceptable flow rates between 0.13 and 3.5 liters per hour. All of the filters examined in these studies were manufactured in the flowerpot shape.

The flow rate can be adjusted in the manufacturing process by increasing the ratio of combustible material (typically rice husk) to clay, by increasing the grain size of combustible used (which will result in larger pore sizes), or by increasing the maximum firing temperature in the kiln (Gensburger, 2011; Bloem et al., 2009). Gensburger's study, which examined filters manufactured in Cambodia, found a linear relationship between flow rate and quantity of rice husk used. The same study found a strong correlation between maximum firing temperature and filter flow rate.

Clearly, the maximum flow rate must be set within a limit that ensures sufficient bacterial removal and turbidity reduction. Bloem et al. (2009) found that an increase in flow rate has no impact on the efficiency of removal of pathogens and that consequently the CDC flow-rate guideline of 1-3 liters per hour was not applicable for pathogen removal. Similarly, a lower flow rate did not generate any improvement in turbidity reduction (Lantagne et al., 2010). Gensburger (2011) further specified that while an increase in flow rate due to a higher combustible content in the filter mix had no negative

impact on bacteria removal, an increase in flow rate due to an increased combustible grain size, and consequent larger pore size, significantly reduced the efficacy of the filter. While a lower flow rate was not found conclusively to improve bacteria removal, a number of studies demonstrated the effectiveness of adding a coating of silver nitrate or colloidal silver to the filter. The addition of this silver significantly improved the LRV of *E. coli* (Bloem et al., 2009; Gensburger, 2011).

While many studies address the implications of flow rate for newly manufactured filters, filter clogging and changes in flow rate and efficacy over time are also of interest. Bloem et al. (2009) investigated their mid-term effects, finding that filters with a higher initial flow rate show a larger decrease in flow rate over a 6-month period, although these filters maintain a higher flow rate than the filters with a lower initial flow rate, with no negative effects on pathogen removal efficiency. While Bloem et al. (2009) did not investigate long-term effects of higher flow rates on pathogen removal efficiency, Brown et al. (2009) performed a study that showed ceramic filters still reducing *E. coli* up to 44 months in use with no relationship between bacteria removal and time in use.

## 1.4 Prior Flow Rate Models

Only a few numerical models have been developed in the past for flow rate through a ceramic filter, and none have focused on the hemispheric filter specifically. Miller (2010) attempted to model flow through a paraboloid-shaped filter by breaking the filter up into three segments and examining the flow through each segment based on Darcy's law. This model allowed him to estimate the hydraulic conductivities of filters tested in the lab, but did not allow for any sensitivity testing. Additionally, because the model split the filter up into large segments, it is by nature only a rough approximation of flow through the filter.

Lantagne (2001) developed a mathematical model based on Eriksen (2001) for flow through a clay pot filter with the goal of determining the maximum allowable hydraulic conductivity of a filter, according to the minimum contact time required for contaminants traveling through the filter to be removed from the water by the filter's silver coating. Darcy's law serves as the basis for this model (as it does for most models of saturated flow in porous media); however, the primary focus of the modeling in this case was the contact time necessary for contaminant removal.

Missing from the prior attempts to model clay pot filters is a model that will allow for easy sensitivity testing to changes in hydraulic conductivity and other parameters. Such a model would need to be sufficiently refined so that any approximations made in the model do not propagate through to the model results. A more refined model would also allow for closer examination of the flow through the ceramic filter and a more robust comparison among filter shapes.

## 1.5 Summary and Application to PHW

Studies conducted in a number of different ceramic filter factories around the world have shown no conclusive effect of filter flow rate on pathogen removal efficiency. Current CDC guidelines, which limit the flow rate to 0.35 liters per hour per liter capacity of the ceramic filter, may therefore be overly conservative. The current PHW standards, which accept filters with flow rates in the range of 3-10 L/hour, while indicative of inconsistencies in the manufacturing process, may not be indicative of inadequate bacteria removal.

Studies conducted in other countries, while informative, cannot provide a comprehensive basis for evaluating the PHW filters. A wide range of production variables, including material selection, clay-to-combustible ratio, mixing process, kiln temperature, and firing times, can impact filter flow rate and efficacy. Research in Nicaragua, Cambodia, and the Dominican Republic shows that hydraulic conductivity and pore size vary significantly based on the type of clay used (Lantagne, 2010), and clay properties will vary from one country to the next. It is therefore necessary to perform additional assessments of the PHW filters themselves in order to assess the impacts of the materials and processes specific to the PHW factory.

As the quality control process continues to be refined, the prior studies discussed in this section provide a foundation for the following questions: 1) Can the cause of the flow rate variability in PHW filters be isolated and the flow rate range refined? 2) Is there a filter shape that may produce a lower variability in flow rate, where the flow rate through that filter is less sensitive to inconsistencies in manufacturing? And 3) Is there a filter shape that produces an optimal flow rate?

This study seeks to address the three questions listed above by developing a model of water flow through each filter shape and simulating flow through the filters for a range of hydraulic conductivities in order to examine the sensitivity of each filter shape to changes in hydraulic conductivity, and also to assess the efficiency of each filter based on the flow rate computed for a given hydraulic conductivity.

# 2 Methods

## 2.1 Flow-Rate Testing

Flow-rate tests were conducted on the hemispheric filter and flowerpot filter in the laboratory at MIT. The hemispheric filter tested was manufactured at the Pure Home Water factory in Ghana, while the flowerpot filter was manufactured in Cambodia. The nature of the numerical model, which is discussed in following sections, requires that these tests be conducted at a constant water level.

In order to conduct the flow-rate tests, it was necessary to place the filter inside a support that would elevate it above the collection vessel and not obstruct flow out of the sides of the filter. The hemispheric filter was placed between two wooden stands above a plastic container, as pictured in Figure 2-1. The flowerpot filter was placed inside of a plastic bucket which had the entire bottom cut out, and this bucket was placed on top of another plastic bucket that collected the water draining from the filter, as seen in Figure 2-2.

Markings were made with a waterproof marker at four intervals on the inner surface of the filter, at locations that corresponded to a certain water height, as measured vertically from the center of the filter. The inside of the hemispheric filter was marked at water levels of 17, 13, 9, and 5 cm, so that a constant water level could be maintained based on visual inspection. The inside of the flowerpot filter was marked at heights of 18, 13, 8, and 3 cm.

**Figure 2-1: Lab testing of hemispheric filter**

**Figure 2-2: Lab testing of flowerpot filter**

The following summarizes the flow-rate testing procedure:

1. Soak filter for 24 hours to ensure saturation.
2. Elevate filter above collection vessel, ensuring that the sides of the filter are unobstructed.
3. Fill filter with water to appropriate water level mark.
4. Set timer for 10 minutes.
5. Place collection vessel underneath filter to catch outflow
6. Allow water to flow through filter, maintaining the initial water level by adding water as necessary.
7. After 15 minutes, measure the volume of water that has been collected in the collection vessel.

This procedure was repeated for all three filter shapes at all marked intervals. Measured water volumes collected after 10 minutes were recorded for all filter shapes at all marked intervals. Based on these measurements, we can calculate a flow rate $Q$ in liters per hour using the relationship:

$$Q = 6V_{10\,min} \qquad 1\text{-}1$$

where $V_{10\ min}$ represents the volume of water collected after 10 minutes of saturated flow through the filter.

## 2.2 Filter Geometry

Measurements for each of the filter shapes were obtained from prior work in Ghana. Flower-pot filter measurements were given by Watters (2010). Paraboloid filter measurements were obtained from Miller (2010), and hemispheric filter shape measurements were obtained from Miller (2012). Images of the flower-pot, paraboloid, and hemisphere filters are shown in Figure 2-3, Figure 2-4, and Figure 2-5, respectively.

**Figure 2-3: Flowerpot filter (image from Watters, 2010)**

**Figure 2-4: Paraboloid filter (image from Miller, 2010)**

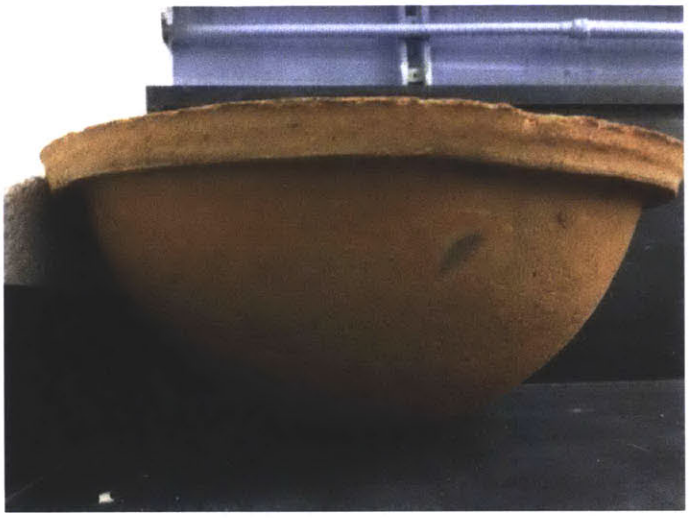

**Figure 2-5: Hemispheric filter**

## 2.3 Model Methodology

As discussed in the introduction, one of the primary goals of this thesis is to develop a model of flow through each of the filter shapes presented in Section 2.2 in order to better understand how the geometry of each filter impacts its flow rate. Rather than developing an analytical model and approximating flow through segments of the filter, we want to run a numerical simulation of flow through the filter that is capable of modeling the geometric irregularities of the various filter shapes, such as the corners of the flowerpot filter, and that will also provide a higher level of accuracy than any hand calculations.

The fundamental transport processes that govern the flow of water through a saturated ceramic filter are the same processes that govern flow through any saturated porous medium, like saturated groundwater flow. Software used for groundwater modeling can therefore easily be adapted to modeling filter flow. FEFLOW, short for Finite Element Flow, is a groundwater modeling software produced by DHI-WASY that can be used for finite-element modeling of flow through porous media (DHI-WASY, 2012). FEFLOW is designed primarily for use in modeling groundwater; however, due to the fundamental similarities between the filter and groundwater flow problems, FEFLOW is already suited to the specific nature of the model used in this study. A finite element model is particularly well-suited to the complicated geometry of the flowerpot shape near its corners.

FEFLOW's primary limitation with respect to the goals of this study is that it is not well-suited for modeling drainage from a filter as a transient flow problem. There is no mechanism in FEFLOW to account for the depletion of water from inside the filter

and the consequent continuous decline in water level. Therefore, in order to model flow through the filter as it drains, we simply simulate steady-state flow through the filter at discrete intervals of water level in the pot, and calculate the flow rate and water-level change over time during the associated discrete time steps. The following sections discuss in detail the process of developing in FEFLOW a model of flow through the ceramic filter. The FEFLOW user manual (DHI-WASY, 2012) provides a complete description of the various capabilities of FEFLOW beyond those discussed in the following sections.

## 2.4 Modeling Filter Shape

In order to develop a model for flow through the filter using FEFLOW, it is necessary to define the region of flow, which in this case is the filter itself. The shape of each filter, barring any slight asymmetry in the filter press, is rotationally symmetric. We can determine three-dimensional flow through the entire filter by modeling flow through one half of a filter cross section in only two dimensions.

The filter measurements in Figures 2-6 through 2-8 were plotted in Excel to produce a two-dimensional cross section of one-half of each filter shape. The x and y coordinates of this cross-section were input into a text file, which was then put into the surface modeling software Surfer, produced by Golden Software (2002), to generate a shapefile for use in the flow model.

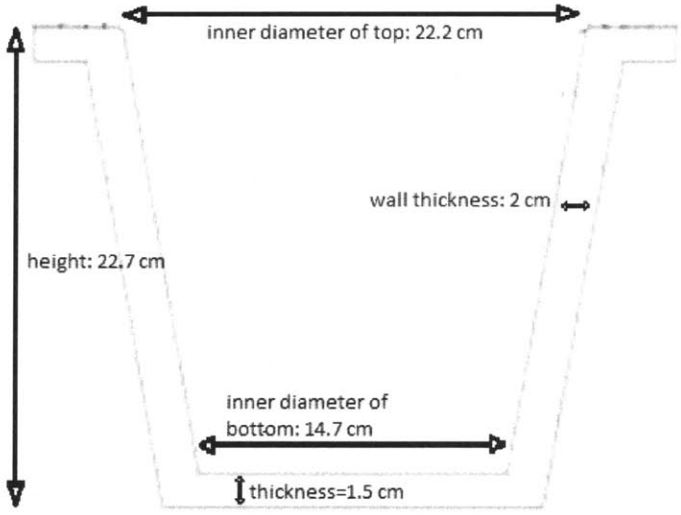


**Figure 2-6: Cross section of flowerpot filter**

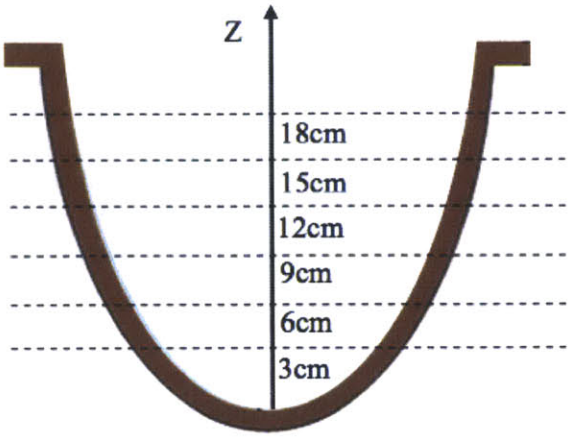


**Figure 2-7: Cross section of paraboloid filter (image from Miller, 2010)**

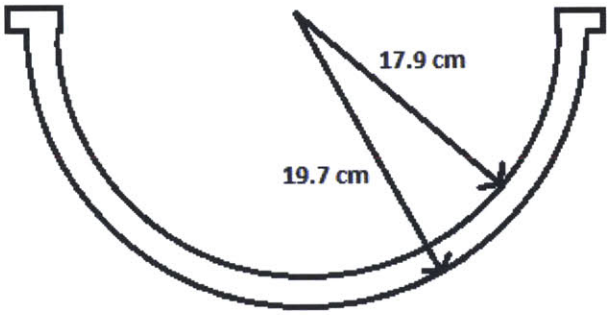


**Figure 2-8: Cross section of hemispheric filter**

The shapefile representing the filter shape was then imported into FEFLOW and used to define the region of flow. In order to develop the basis for a finite-element flow model, it is necessary to divide the flow region into a finite-element grid. The FEFLOW user interface contains an automatic grid generator that divides a given shapefile into a finite-element grid according to one of several user-selectable algorithms m.

GridBuilder, the algorithm used for the flowerpot and hemispheric shape, generates a triangular grid with a user-specified number of elements. The Advancing Front algorithm was used to generate a similar grid for the paraboloid filters. Both algorithms generate a similar triangular grid; the Advancing Front algorithm was used for the paraboloid shape because the GridBuilder algorithm failed to generate a grid for the paraboloid geometry.

## 2.5 Model Settings

After generating the finite element grid, we specify the general model configuration, boundary conditions, parameter values, and other settings. The model settings include the direction of gravity, the saturation of the porous medium, and the state of flow (steady or transient). In this case, we are modeling steady flow out of a fully saturated filter. With the 2-dimensional cross section, the problem is defined in FEFLOW as being rotationally symmetric about the vertical axis. We then specify a hydraulic conductivity and porosity for the filter flow model. The model was run for a hydraulic conductivity of 0.234 cm/hr (the value obtained by Miller, 2010), and for values of 0.42 and 0.83 cm/hr in order to conduct a sensitivity analysis. The porosity was set at 0.45 (based on Miller, 2010).

The inner and outer surfaces of the filter are both subject to constant-head boundary conditions. Hydraulic head $h(z)$ as a function of elevation is defined as:

$$h(z) = \frac{P}{\rho g} + z \qquad 2\text{-}1$$

where $z$ is the elevation above the zero datum (which we choose to be the bottom of the outside of the filter), $P$ is the pressure at that elevation , $\rho$ is the density of the water in the filter, and $g$ is the acceleration due to gravity. We assume hydrostatic pressure in the filter in determining the value of $P$. With hydrostatic pressure in the filter, the pressure $P$ at a given depth $d$ below the water surface is given by:

$$P = \rho g d \qquad 2\text{-}2$$

The equation for head $h_i(z)$ along the inner filter surface then simplifies to:

$$h_i(z) = d + z \qquad 2\text{-}3$$

At any given point, the depth $d$ of the water above that point can be found by subtracting the elevation $z$ from the total height $H$ of the water in the filter. Therefore, along the inner surface of the filter, the sum of $d$ and $z$, and consequently the value for $h_i(z)$ in Equation 2-3, will be constant and equal to the height $H$ of water in the filter.

$$h_i(z) = H \qquad 2\text{-}4$$

The outside surface of the filter, as a free surface exposed to atmospheric pressure, will have zero pressure at all points on the surface, $P = 0$. The value for $h\ (z)$ on the outer surface of the filter therefore reduces to:

$$h(z) = z \qquad 2\text{-}5$$

The head boundary conditions represented by Equations 2-4 and 2-5 were specified in FEFLOW by assigning appropriate head values to each node of the outer surface, equal to the elevation of that node, and a constant head over the inner surface equal to the specified, fixed height of water in the filter.

## 2.6 Steady-State Flow Model

We begin by modeling flow through the saturated filter when it is full of water. Saturated flow is described by a continuity equation following Darcy's law:

$$q = -K\frac{dh}{dl}\hat{n} \qquad 2\text{-}6$$

where K is the hydraulic conductivity of the ceramic filter, $\frac{dh}{dl}$ represents the head gradient across the thickness of the filter, and $\hat{n}$ is the outward unit vector normal to the filter surface, representing the direction of flow. The head gradient $\frac{dh}{dl}$ can be approximated as:

$$\frac{dh}{dl} = \frac{h_i - h_o}{b} \qquad 2\text{-}7$$

where $h_i$ and $h_o$ represent the head at the inner and outer surfaces of the filter, respectively, and $b$ is the thickness of the filter. Thus, normal flux $q$ out of the filter is computed as follows:

$$q(z) = -K\left(\frac{z-H}{b}\right)\hat{n} \qquad 2\text{-}8$$

Equation 2-8, based on Darcy's Law and the constant-head boundary conditions specific to the filter, forms the basis of the model calculations. The value of $q$ will be computed by FEFLOW at each node of the finite element grid, and we can take the sum of all fluxes $q$ for each node along the filter's outer boundary to find the total flow $Q$ out of the filter.

## 2.7 Transient flow model

Because FEFLOW is designed primarily for use with groundwater and therefore is not capable of modeling the drainage of the ponded "surface water" inside the ceramic filter as the filter empties, we establish a stepwise transient flow model using results from the steady-state model over discrete time intervals. Modeling steady flow over a range of water heights, from full to empty, will allow us to develop a relationship between flow rate and height. We can use the computed flow rate at a given height over a discrete time step $\Delta t$ to estimate the volume $V$ drained during that time step:

$$V = Q\Delta t \qquad 2\text{-}9$$

where $Q$ is the computed flow rate out of the filter. We can then use this value to determine the new height of water in the filter for the subsequent time step. The relationship between the volume $V$ drained during a time step and the change in water height depends upon the filter geometry.

***Flow Rate Calculation***

After running a steady-state simulation in FEFLOW of flow through the flowerpot filter with a constant water level, the Darcy flux $q$ out of each finite element is computed. FEFLOW also computes the flow rate $Q$ out of a selected boundary. Given

the Darcy flux $q_i$ at a given node $i$, computed in FEFLOW, the total flow rate $Q$ out of the filter is also computed by FEFLOW using a discrete summation of the general form:

$$Q = \sum_i q_i \Delta A_i \qquad 2\text{-}10$$

where $\Delta A_i$ represents the discrete surface area of the filter which is subject to flux $q_i$.

***Head Drop Calculation***

As discussed above, the change in filter water height generated by flow rate $Q$ over a time interval $\Delta t$ depends on the geometry of the filter. Watters (2011) provided a schematic of the flowerpot filter dimensions which enables us to compute the volume of a given filter segment. The following relationship exists radius $r$ and height $z$, both in centimeters, along the inner surface of the pot sides, with (0,0) defined for this purpose as the center of the inner face of the pot bottom:

$$r = 0.1769z + 7.35 \qquad 2\text{-}11$$

Dimensions for the paraboloid filter are given by Miller (2010):

$$r = 2.685\sqrt{z} \qquad 2\text{-}12$$

Finally, the hemispheric filter is reported by Miller (2012) to have an inner radius of 17.9 centimeters and an outer radius of 19.69 cm. Figures 2-6 through 2-8 show cross sections of each filter shape. We can make use of these dimensions to calculate the change in height associated with the computed change in volume over a given time step. Full derivations of the head drop calculations for the flowerpot, paraboloid, and hemispheric filters are given in Appendices B, D, and F, respectively.

# 3 Results & Discussion

## 3.1 Lab Testing

Tables 3-1 and 3-2 summarize the measured flow rate for each filter shape at each designated water height, and these values are plotted in Figure 3-1. It is evident from Figure 3-1 that the hemispheric filter produces a larger flow rate at a given height, and that the flow rate increases more quickly with increasing height. However, the conductivities of these two filters are unknown. In order to determine the conductivity of each filter and assess its "efficiency" with regards to flow performance, it is necessary to examine the results of the numerical models over a range of hydraulic conductivities, which is done in Section 3.4 of this thesis.

**Table 3-1: Flowerpot lab test results**

| Water height [cm] | Amount collected after 10 minutes [mL] | Flow rate [L/hr] |
|---|---|---|
| 23.0 | 600 | 3.60 |
| 20.0 | 400 | 2.64 |
| 15.0 | 240 | 1.44 |
| 10.0 | 125 | 0.75 |
| 5.0 | 55 | 0.33 |

**Table 3-2: Hemisphere lab test results**

| Water height [cm] | Amount collected after 10 minutes [mL] | Flow rate [L/hr] |
|---|---|---|
| 18.5 | 985 | 5.91 |
| 14.5 | 550 | 3.30 |
| 10.5 | 275 | 1.65 |
| 6.5 | 130 | 0.78 |

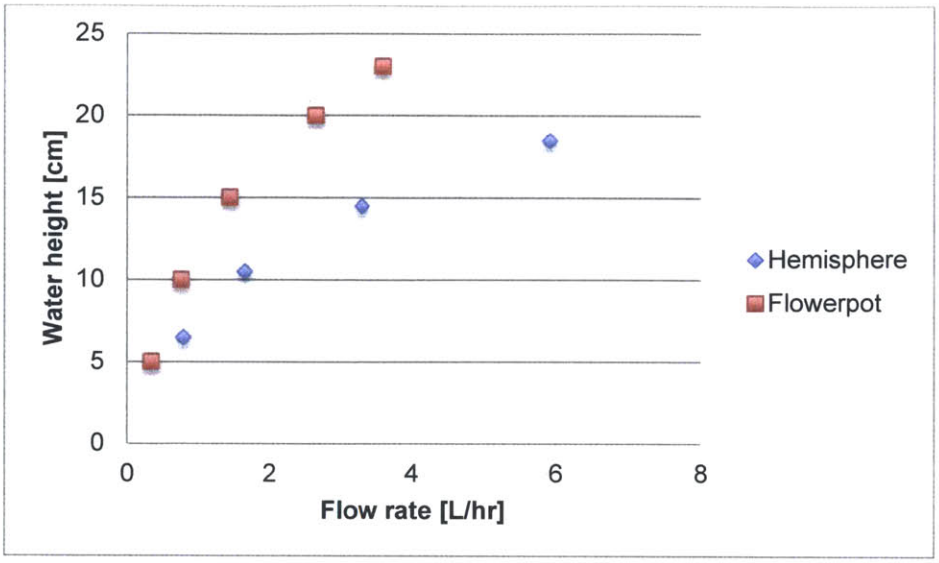


**Figure 3-1: Lab test tesults: Flow rate versus water height for flowerpot and hemispheric filters.**

## 3.2 Numerical Modeling

One output of the steady-state model is a map of the distribution of hydraulic head in the filter cross section for each filter shape. Figures 3-2, 3-3, and 3-4 show the hydraulic head distribution in the flowerpot, paraboloid, and hemispheric filter shapes, respectively, for the scenario in which the pot is full. We can use these images to predict the comparative performance of the filter shapes with respect to flow rate. Because flow rate is driven by the conductivity and head gradient in a medium, and the filters in question have the same model conductivity value, hydraulic head gradient is the only driving force for flux out of the filter. It is evident from these images that, while all filters have a nearly identical flux at the bottom of the filter (varying only slightly based on the thickness of the filter at that point), the steep sides of the flowerpot cause its head gradient to drop off quickly with increasing height. The hemispheric filter, on the other hand, due to its less steeply sloped sides, experiences a greater head gradient across more of its surface area. We can therefore expect that this filter shape will produce a greater flux over a larger proportion of its area, and therefore have a higher flow rate for a given water height.

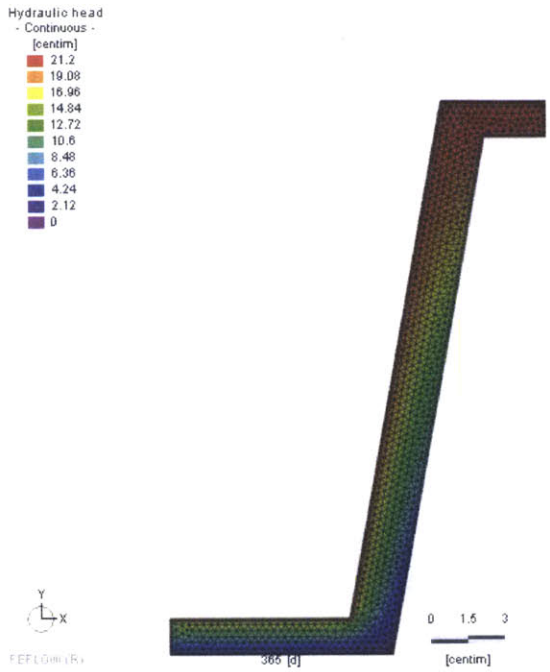


**Figure 3-2: Hydraulic head distribution in full flowerpot filter**

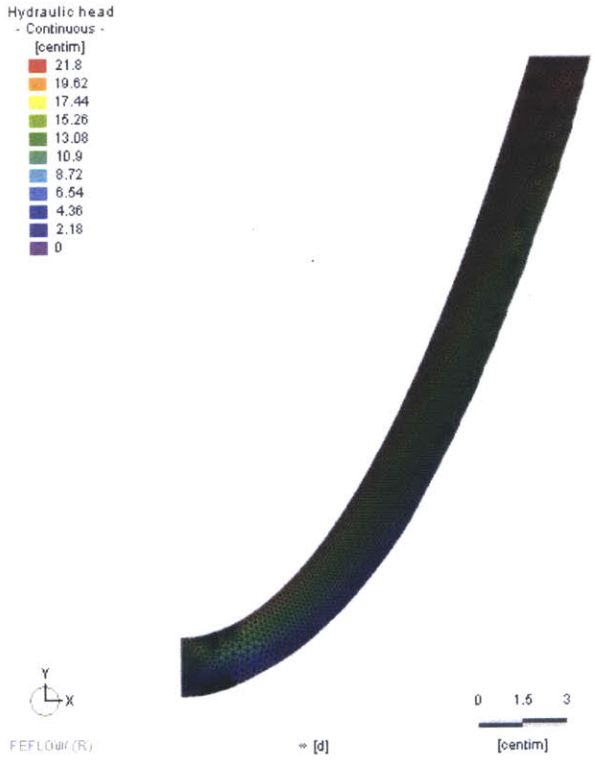


**Figure 3-3: Hydraulic head distribution in full paraboloid filter.**

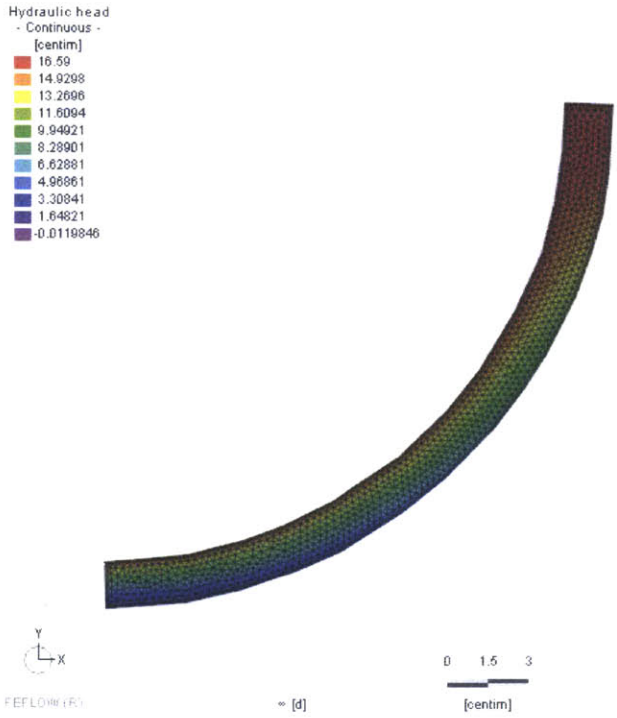


**Figure 3-4: Hydraulic head distribution in full hemispheric filter.**

The head distribution shown in Figures 3-2, 3-3, and 3-4 is the driving force behind the flow of water out of the filter. Figures 3-5 through 3-7 show the Darcy flux, $q$, in the filter cross-section for each filter shape, for a conductivity of 10 cm/day. It is clear from comparing the Darcy flux distribution in each filter that the hemispheric filter has a larger flux over more of its exterior surface area. It is also interesting to note the flux distribution at the corners of the flowerpot: while the highest flux over the entire area occurs at the inner corners, the flow is dispersed over the rapidly expanding corner area so that the flux emerging from the outer surface of the corner is lower than the flux over the rest of the outer surface.

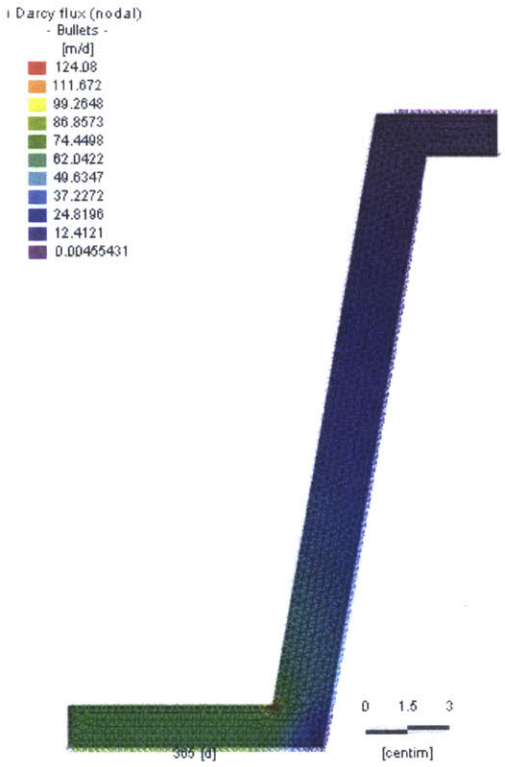


**Figure 3-5: Darcy flux in full flowerpot filter**

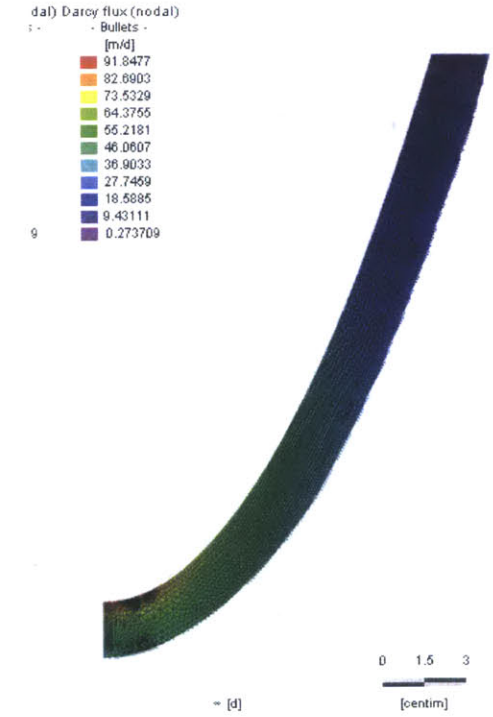


**Figure 3-6: Darcy flux in full paraboloid filter.**

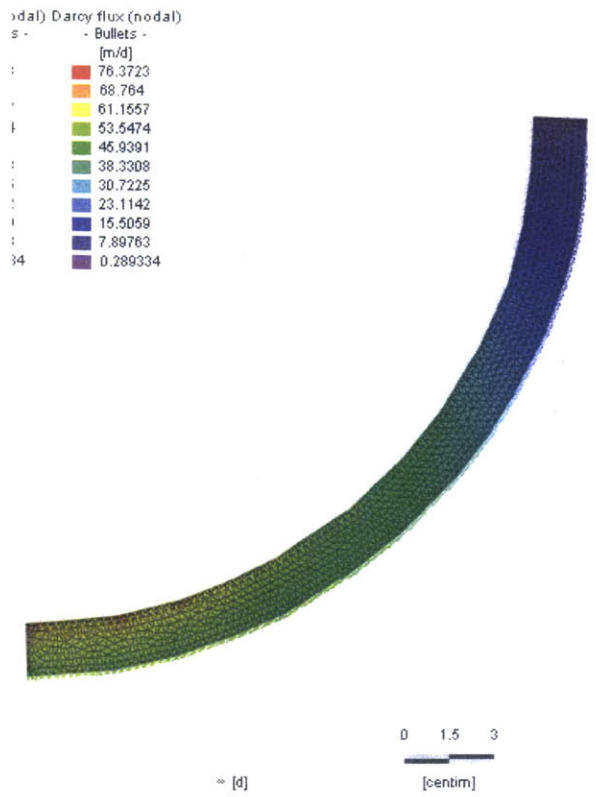


**Figure 3-7: Darcy flux in full hemispheric filter.**

## 3.3 Flow Rate Variation with Water Height

For each shape, the modeled flow rate results are graphed with respect to water height, for all modeled values of hydraulic conductivity. These graphs are shown in Figures 3-8 through 3-10. The general and immediately observable trends displayed in the plots of flow rate versus water height are that the flow rate of a filter increases with height, and that the highest flow rates occur when the filter is fuller, dropping off to much lower levels when the water is at a depth of about 5 centimeters. We can also observe from these graphs that as the value of hydraulic conductivity increases, the difference in flow rate performance amount the paraboloid, flowerpot, and hemispheric filters also increases. At the lowest hydraulic conductivity value, for example, the "full" flow rate of the hemispheric filter is greater than that of the flower pot by approximately 2 liters, while at the highest value of hydraulic conductivity this difference has increased to just over 6 liters.

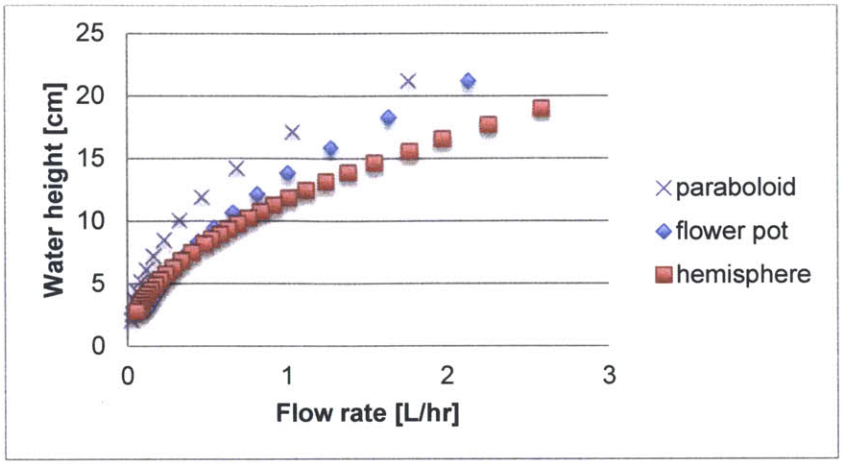


**Figure 3-8: Modeled flow rate versus water height for flowerpot, paraboloid, and hemispheric filters, K = 0.234 cm/hr.**

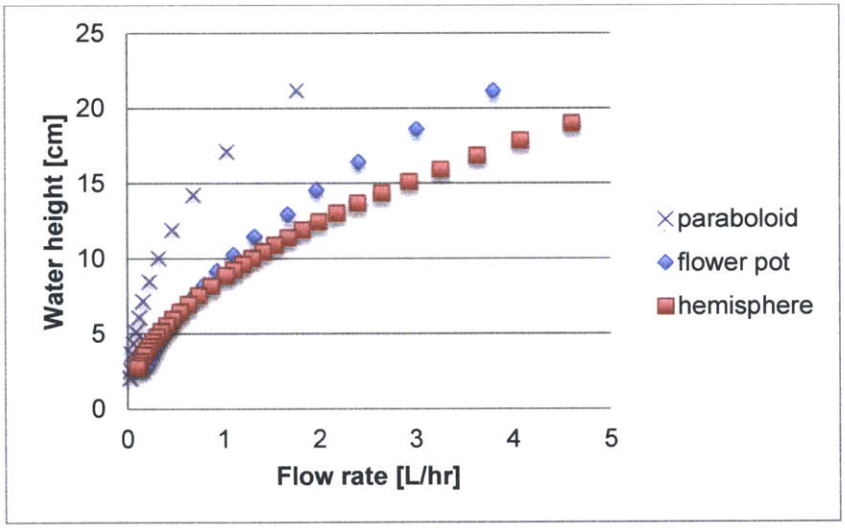


**Figure 3-9: Modeled flow rate versus water height for flowerpot, paraboloid, and hemispheric filters, K = 0.42 cm/hr.**

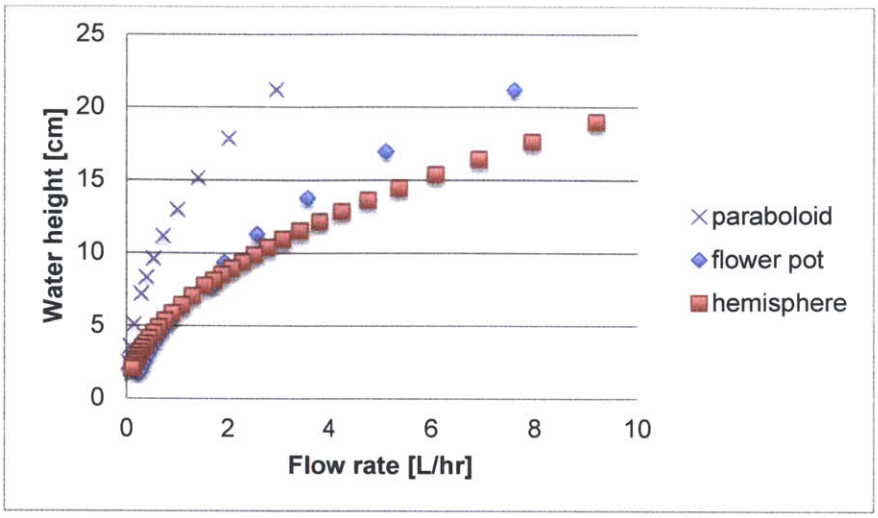


**Figure 3-10: Modeled flow rate versus water height for flowerpot, paraboloid, and hemispheric filters, K = 0.83 cm/hr.**

Based on the observed flow rate in the filter, we can calculate an average travel time $T$ for a particle passing through the filter. This time can be calculated as:

$$T = \frac{V_F}{Q} \qquad 3\text{-}1$$

where $V_F$ is the volume of the filter media. It should be noted that this $T$ gives an *average* travel time. Due to the lower head gradient near the top of the filter, the travel time for a given particle will be longer if that particle passes through the sides of the filter nearer to the top, and shorter if the particle passes through the bottom of the filter. Additionally, the calculated travel time does not take into account the presence of the silver nitrate filter coating, which will retard the transport of contaminants through the filter. The travel time of water through the filter will be the shortest when the filter is fullest, so by calculating $T$ based on $Q$ for a full filter, we can establish the "weakest" performance level of the filter in terms of contaminant removal.

## 3.4 Parameter Sensitivity Testing

In order to test the sensitivity of the flow models to changes in hydraulic conductivity and examine the variation of this sensitivity among filter shapes, each model was run with three different values of hydraulic conductivity. Appendix A contains the complete set of model results from this sensitivity testing.

### 3.4.1 Flower Pot Filter

Figure 3-11 contains a graph of the numerical results for flow rate through the flowerpot filter with three different values of hydraulic conductivity. The results of the laboratory flow-rate testing are shown on the plot as well for comparison. In this graph,

we can observe a consistent relationship between flow rate $Q$ and water height $h$. For the flowerpot filter, flow rate is quadratically related to height, and the coefficients of this polynomial expression are proportional to the hydraulic conductivity, $K$. Figure 3-12 shows a graph of the x-squared coefficient, $a$, versus $K$, and of the $x$ coefficient $b$, versus $K$. This strong correlation leads us to the conclusion that if the flow rate $Q$ can be measured at a given $h$ for a flowerpot filter, then the hydraulic conductivity $K$ of that filter can be calculated from the relationship given by the graph above, *assuming that the flow rate at a height of zero is equal to zero.* This assumption, which is reasonable as a water height of zero will not generate any head gradient to drive flow, allows us to simplify the slope of the line to the ratio of $Q$ to $h$.

$$Q = 0.015Kh^2 + 0.12Kh \qquad 3\text{-}2$$

All equations in this section assume that flow rate is given in liters per hour, height in centimeters, and hydraulic conductivity in centimeters per hour. A similar analysis was conducted for the paraboloid and hemispheric filters, as discussed in the Sections 3.4.2 and 3.4.3.

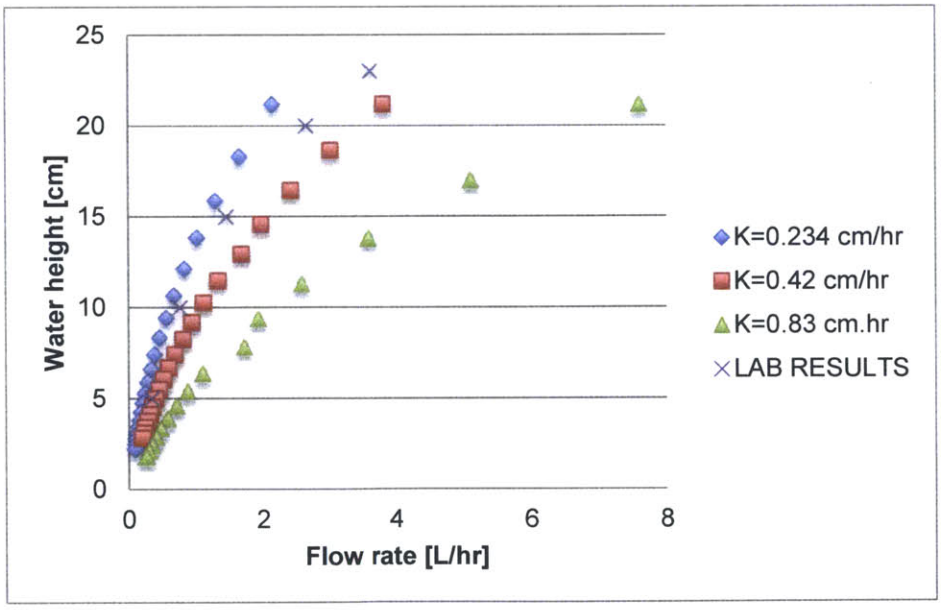


**Figure 3-11: Flow rate versus water height in flowerpot filter, model and lab results**

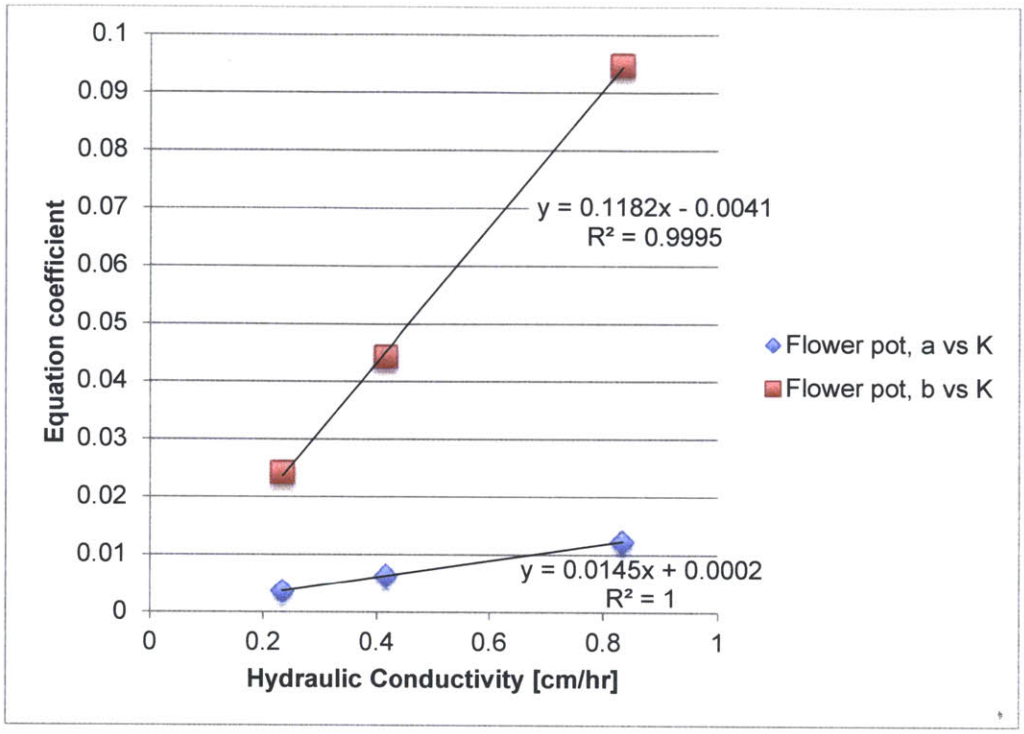


**Figure 3-12: Coefficients of flowerpot Q-h relationship vs. hydraulic conductivity.**

### 3.4.2 Paraboloid Filter

A graph of flow rate as a function of water height in the paraboloid filter is shown in Figure 3-13, again for three different hydraulic conductivities.

For the paraboloid filter, the relationship between flow rate $Q$ and water height $h$ is parabolic of the form:

$$Q = ah^2 + bh \qquad 3\text{-}3$$

where $a$ and $b$ are constants. A strong correlation exists between $a$ and $K$, of the form:

$$a = 0.19K \qquad 3\text{-}4$$

### 3.4.3 Hemispheric Filter

Finally, Figure 3-14 shows the results for the modeled flow rate versus water height in the hemispheric filter. For the hemispheric filter, the same general form parabolic relationship exists between $Q$ and $h$ as for the paraboloid filter. However, a fitted plot of $a$ against $K$ shows that the relationship between these two variables is given by:

$$a = 0.03K \qquad 3\text{-}5$$

and the relationship between $b$ and $K$ is given by:

$$b = .006K$$

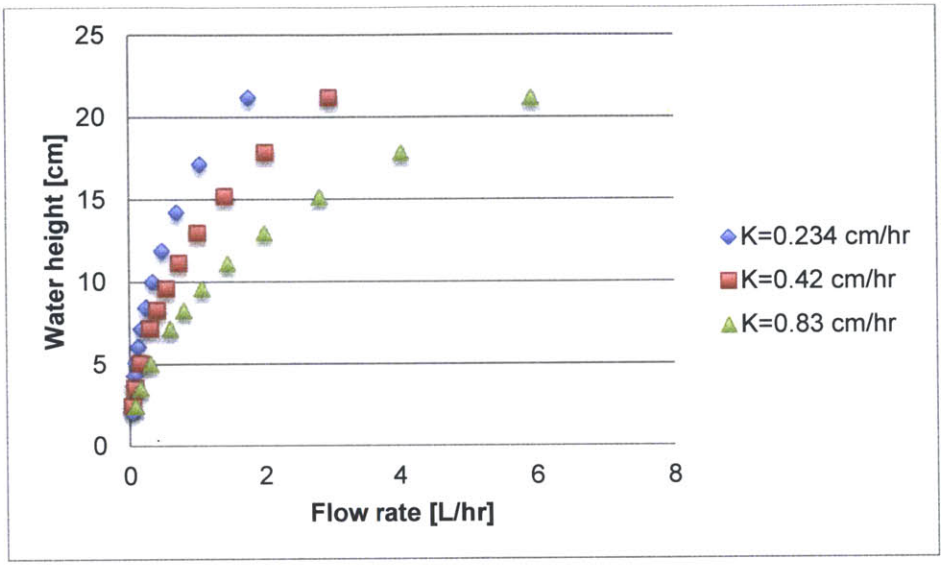


**Figure 3-13: Modeled flow rate versus height in paraboloid filter.**

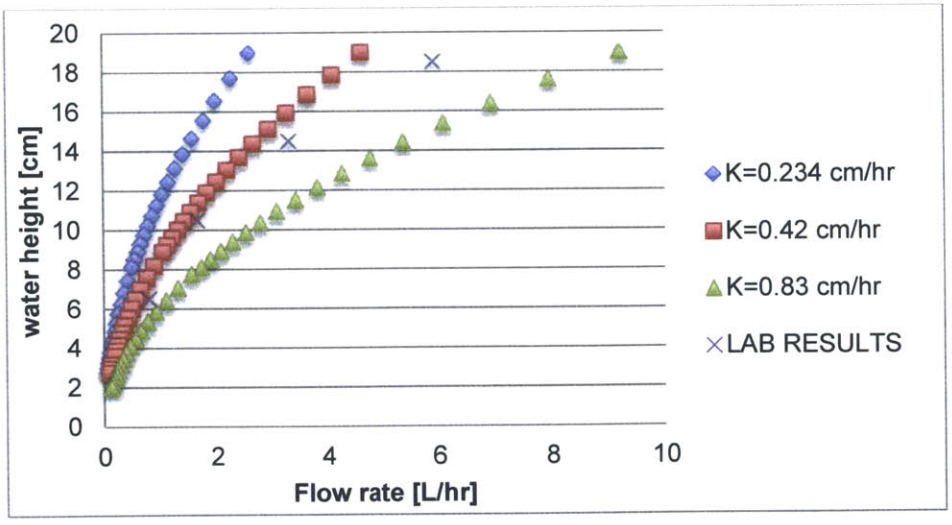


**Figure 3-14: Flow rate versus height for hemispheric filter, modeled and lab results.**

### 3.4.4 Shape Comparison

The sensitivity analysis discussed in Sections 3.4.1, 3.4.2, and 3.4.3 indicates that the relationship between flow rate and height is strongly correlated with hydraulic conductivity for all filter shapes, while the nature of that correlation varies. A change in $K$ will generate changes of different magnitude in the flow through the filter depending on the shape of the filter. Figure 3-15 shows a plot of the derivative of flow rate, $Q$, with respect to $K$, over the range of possible water heights in each filter. It is evident from this graph that the flow rate through the hemispheric filter shape is almost 50% more sensitive to changes in $K$ when full. As the filters drain and the water level falls, the hemispheric filter continues to be more sensitive than the flowerpot filter to hydraulic conductivity, until the height diminishes to around six centimeters, where the flow rate is very small in both filters.

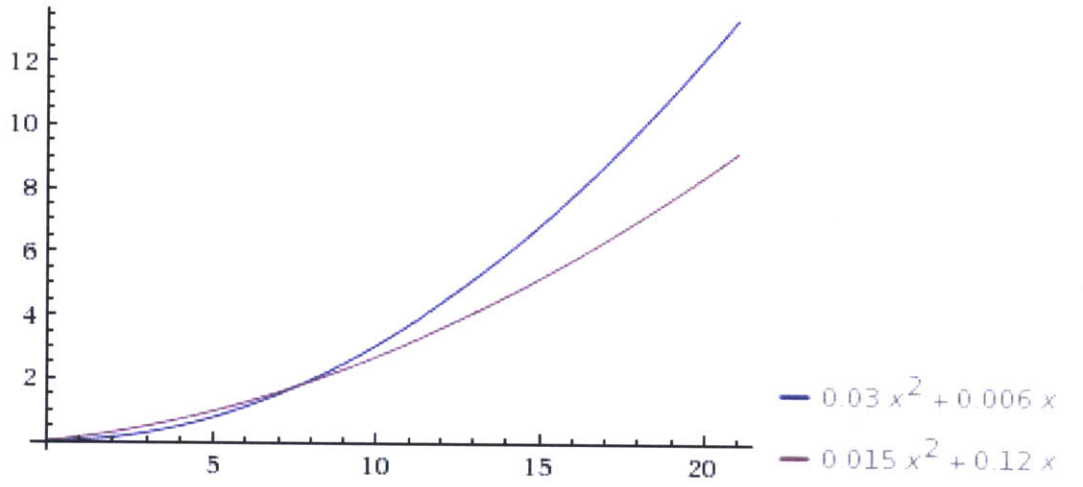


**Figure 3-15: dQ/dK versus water height for flower pot (purple) and hemispheric (blue) filters (image courtesy of Wolfram Alpha)**

Because the numerical models are based on actual dimensions of filters manufactured in the PHW factory, the results of the model can be used to estimate the hydraulic conductivity of a given filter. Once a flow rate $Q$ is observed at a given height $h$, as was done for the flower pot filter above, the relationships established among $Q$, $h$, and $K$ will allow for easy calculation of filter hydraulic conductivity. It is important to note, however, that the relationships determined in this thesis are valid *only* for the filter geometries specified. Any change in the relationship between radius and height for a filter shape will result in the model no longer being applicable to that new filter, and a new model will need to be established.

## 3.5 Flow Rate Variation with Time

It is important to understand how the flow rate through a filter changes over time. The results of the numerical modeling allow for an approximation of flow rate over time, based on the selected time step $\Delta t$.

### 3.5.1 Flower Pot Filter

The results of the modeled flow rate over time are plotted in Figure 3-16. For the flowerpot filter, the relationship between flow rate $Q$ and time $t$ is exponential of the form:

$$Q = ce^{-kt} \tag{3-6}$$

where $c$ and $k$ are constants. A strong correlation exists between $c$ and $K$, of the form:

$$c = 9.4\sqrt{K} - 2.95 \tag{3-7}$$

and $k$ and $K$ are also related, by the equation:

$$k = 1.45K \tag{3-8}$$

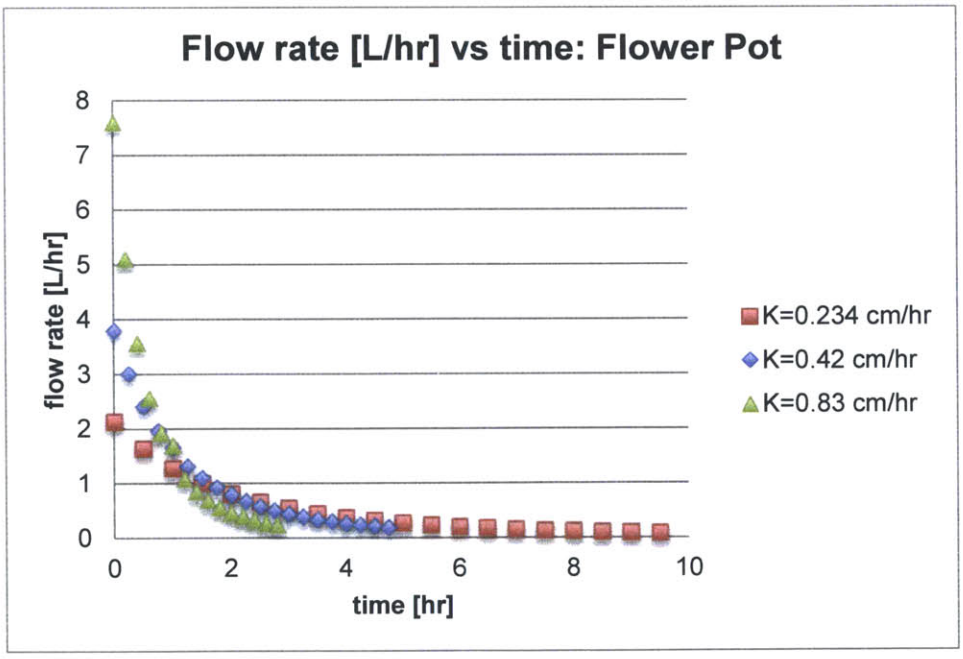


**Figure 3-16: Modeled flow rate versus time, flowerpot filter.**

### 3.5.2 Paraboloid Filter

Flow through the paraboloid filter varies exponentially over time, as shown in Figure 3-17. The general equation for flow rate $Q$ versus time $t$ through the paraboloid filter is given by:

$$Q = ce^{-kt} \tag{3-9}$$

where $c$ and $k$ are both constants. Similarly to the flowerpot filter, the following relationships can be established between the constants in Equation 3-9 and the hydraulic conductivity, $K$, in centimeters per hour:

$$c = 6.65K \tag{3-10}$$

and

$$k = 1.57K \tag{3-11}$$

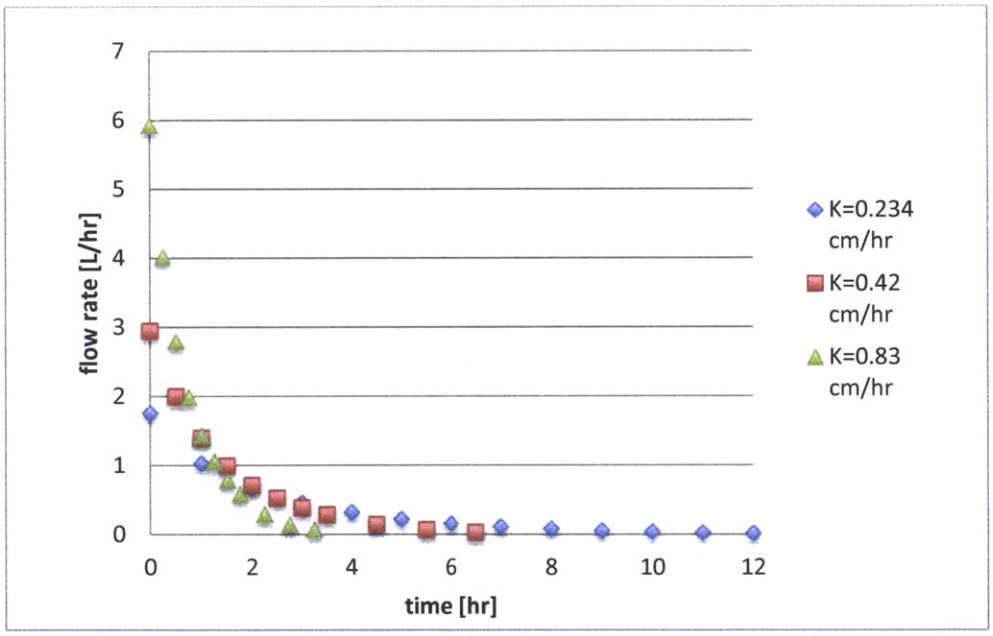


**Figure 3-17: Modeled flow rate versus time, paraboloid filter.**

### 3.5.3 Hemispheric Filter

The variation of flow rate over time in the hemispheric filter is, similarly to the paraboloid filter, exponential, as seen in Figure 3-18. Like the paraboloid filter, the equation for flow rate over time is of the general form:

$$Q = ce^{-kt} \tag{3-12}$$

where $c$ and $k$ are both constants. However, the relationships between the constants in the equation and the hydraulic conductivity, $K$, are slightly different:

$$c = 12.3\sqrt{K} - 3.92 \qquad 3\text{-}13$$

and

$$k = 0.74K \qquad 3\text{-}14$$

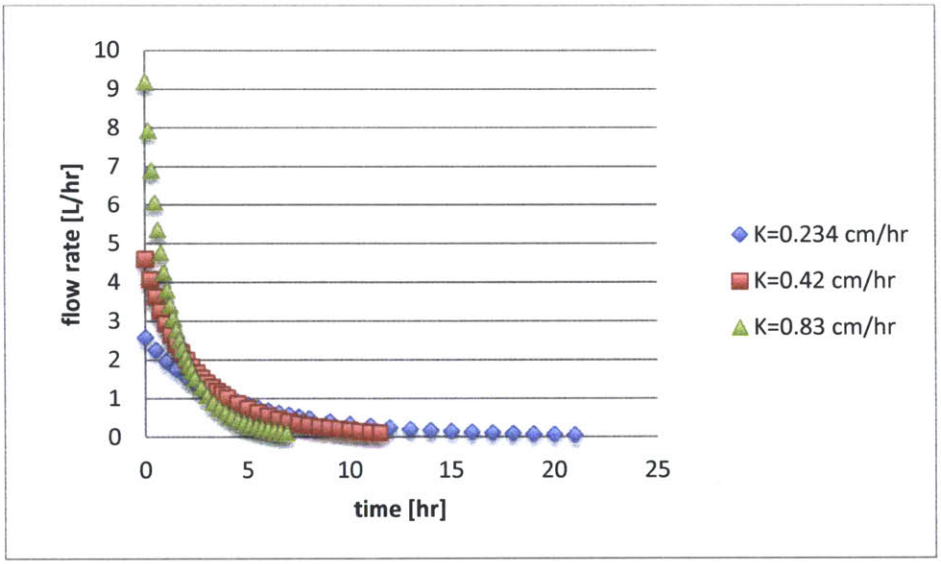


**Figure 3-18: Modeled flow rate versus time, hemispheric filter.**

### 3.5.4 Discussion of Flow Rate vs Time Results

Understanding how the flow rate through a filter varies over time is critical to assessing the performance of that filter. The flow rate must, of course, be slow enough to allow adequate contaminant filtration, but must also be quick enough to provide the user(s) of the filter with an adequate supply of filtered water.

When factories such as the PHW factory perform flow rate tests, the results are typically reported in liters per hour, where this number is obtained simply by measuring the amount of water filtered in the first hour of flow through a saturated filter, starting when the filter is full. It is evident from the graphs above that this number is not an accurate representation of the flow rate. Figures 3-18, 3-19, and 3-20 show a "zoomed in" version of the modeled flow rate over time plots for each filter shape, focused on the first three hours of flow. These graphs can allow us to draw several important conclusions relevant to filter performance. Firstly, it is clear that most of the flow through the filter occurs during the first three hours of use, assuming that the filter is saturated at

the starting point. From a practical standpoint, this means that if a family fills the filter and waits for it to drain completely before refilling it, they are not using the filter to its full potential. After about three hours, the flow rate is reduced to an insignificant level.

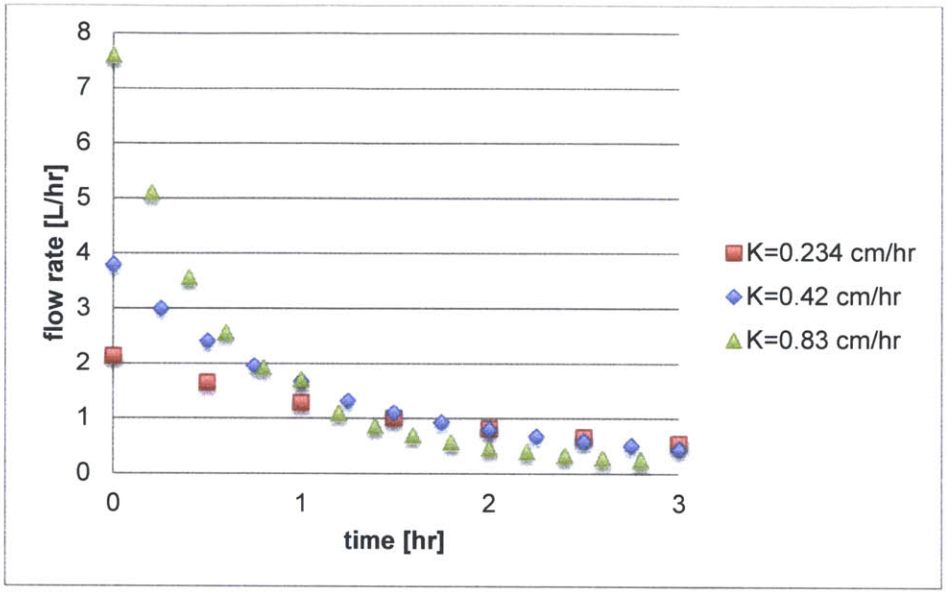


**Figure 3-19: Modeled flow in flowerpot filter over first three hours.**

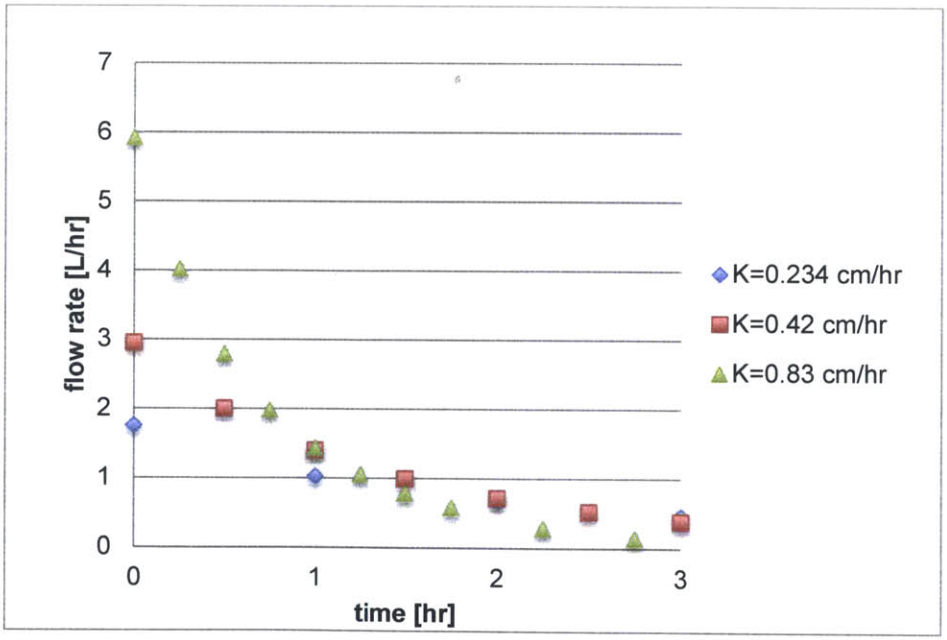


**Figure 3-20: Modeled flow in paraboloid filter over first three hours.**

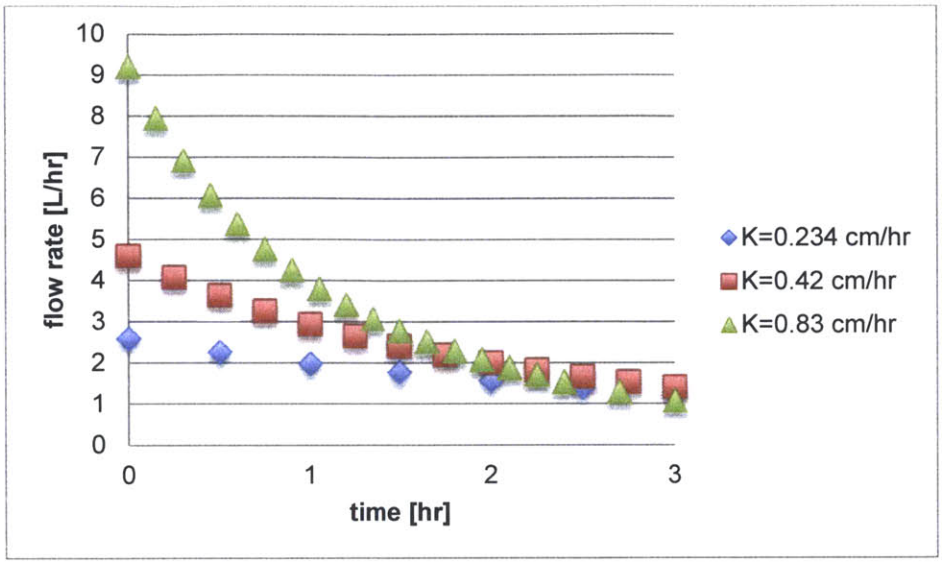


**Figure 3-21: Modeled flow in hemispheric filter over first three hours.**

It is also evident from the graphs that the flow rate during the first hour is much greater than that over any subsequent time period. The factory control tests which record the volume of water filtered during the first hour are in fact reporting the area under the above curves between $t$=0 and $t$=1. The primary problem with this reporting method is that it could present users with an inaccurate picture of the level of performance they can expect from their filter. A starting flow rate of 2 liters per hour does not mean that the filter will then filter 4 liters of water in 2 hours. We can see that the flow produced during the second hour is less than half of the flow produced during the first hour for all three filter shapes. Additionally, integrating the flow rate over the first hour for the hemispheric and flower pot shapes reveals that the reported value is much higher for the hemispheric than for the paraboloid filter, and the difference between the reported values will increase as K increases.

## 3.6 Model Limitations

It is important to note the limitations of the numerical model developed in this thesis in estimating the flow rate over time for a given filter shape. Because the model was developed as a sequence of steady-state flow rates over discrete time intervals, the flow rate $Q$ drops off more quickly over time in the model than it does in reality. Because we are assuming a constant flow rate $Q$ over a time interval of between 15 and 60 minutes, we overestimate the change in volume and therefore the head drop that occurs over that time, arriving at a lower water level and therefore lower flow rate more quickly than in reality, in which $Q$ is actually decreasing over the specified time interval and therefore generating a smaller volume change and smaller head drop. However, this

approximation does not extend to the change in flow rate with water height, as these values were calculated instantaneously and are independent of time. The relationships developed for these parameters are therefore not subject to the same limitations.

# 4 Conclusions and Recommendations

The following research goals were accomplished in this study:

1. Finite-element models were developed for flow through flowerpot-, paraboloid-, and hemispheric-shaped clay pot filters.
2. Comparison of the flow through these filter shapes revealed that the hemispheric filter provides the highest flow rate for a given hydraulic conductivity and porosity.
3. Sensitivity testing revealed that a gentler slope and greater curvature of the filter leads to higher sensitivity of flow rate to hydraulic conductivity. The flowerpot shape is therefore least sensitive to changes in hydraulic conductivity and the hemispheric shape is most highly sensitive to those changes.

The PHW factory has been experiencing significant variability when conducting laboratory flow-rate tests for quality assurance, observing flow rates up to 10 liters per hour whereas the global norm falls between 1 to 2.5 liters per hour. However, most filter factories around the world have continued to manufacture the flowerpot filter, while PHW has been producing a hemispheric filter. Thus, the discrepancy in flow-rate test results may be attributable to the naturally greater variability in flow rate of the hemispheric shape as compared to the flowerpot shape, as well as the increased sensitivity of this shape to changes in hydraulic conductivity. Inconsistencies in manufacturing such as kiln temperature distribution or inhomogeneous mixing of the clay mix will produce a range of hydraulic conductivities for a given filter batch. This variability in hydraulic conductivity will produce a wider range of flow rates for the hemispheric shape than for the flowerpot shape, due to its higher sensitivity to changes in hydraulic conductivity.

## 4.1 Research Recommendations

One of the approximations made in this study is the discretization of the drainage through the filter, which resulted in a consistent underestimate of the filter flow rate over time due to the overestimation of the volume of water drained over a given discrete time step. While the instantaneous flow rate results for a given height are accurate because they are independent of time, refining the estimation of flow rate over time will allow for a better estimate of the filter's "useful" filtering time—the number of hours over which the filter will be filtering a non-negligible amount of water, which in turn will allow manufacturers to provide families with estimates of the time interval after which it is useful to refill their filter.

While this study has investigated flow rate through different filter shapes, it would be valuable to develop a model for the travel time through a filter, which is important in understanding the filter's biological removal effectiveness. In order to

develop this model, it is necessary to investigate the relationship between hydraulic conductivity and porosity for each filter, and determine if this relationship is consistent among filters manufactured in the same factory and if it varies among the different filter shapes. While the collection of factory data can be useful in determining the set of factors which impact this relationship, the development of a numerical model can be a useful tool in understanding this relationship and how it impacts the overall performance of a filter.

This model could then be used in conjunction with the results of this study to assess filter performance: this study provides a means of estimating a filter's conductivity given its initial "full" flow rate, and that conductivity value could be used, once a relationship has been determined, to estimate a filter's porosity and thereby establish the travel time of a contaminants through the filter. These parameters can then be assessed independently of the filter composition, which will not only render the model valuable to factories around the world, but will also allow for the easy determination of the impact of filter composition and other manufacturing variables on filter hydraulic conductivity and porosity.

## 4.2 Recommendations for Pure Home Water

Based on this study, several recommendations can be made to Pure Home Water regarding their current and future manufacturing and quality control processes. Firstly, after comparing the performance of the three filter shapes, it is evident that the hemispheric filter is the most efficient, producing the greatest flow rate for a given value of hydraulic conductivity. In general, this filter is capable of removing biological contaminants with equal effectiveness as other shapes while doing so for a greater volume of water at once.

Secondly, an issue of concern at the factory is that the hemispheric filters currently being produced are operating at a wide range of flow rates, between 2 and 10 liters per hour, while the globally accepted norm is much lower, between 1 and 3 liters per hour. The results of this study suggest that this variability may in fact have nothing to do with manufacturing issues at the factory; rather, the hemispheric filter, due to its shape, will naturally generate a higher flow rate at a given hydraulic conductivity than the flowerpot filter. Because the flowerpot filter is the standard manufactured shape around the world for which the standard flow rate range was established, while the hemispheric filter shape is the model currently being produced at the PHW factory, it may not be reasonable to compare the quality control standards of other factories to those of PHW.

The wider range of flow rate can be explained by the hemispheric filter's higher sensitivity to changes in hydraulic conductivity. Because the manufacturing process is subject to inconsistencies in material quality, grain size, mixing of the clay, kiln temperature distribution, mold pressure, and other factors that can cause variations in

hydraulic conductivity, no factory is capable of producing filters with perfectly consistent hydraulic conductivities. However, if we assume that the ceramic filter factories around the world experience similar manufacturing inconsistencies that will generate similar variations in hydraulic conductivity, we can then also conclude that these discrepancies will generate a larger variation in flow rate for the hemispheric shape than for the flowerpot shape. In short, the variability in flow rate is not indicative of any manufacturing issue or filter inefficacy specific to PHW, but is simply a product of the choice of filter shape.

PHW has also developed a "first drip" test that measures the travel time of a drop of water through the filter. This test measures the amount of time that it takes for the first drop of water to emerge from an unsaturated filter when full. This test on its own may not be an accurate indicator of flow rate, as it measures the travel time through an *unsaturated* filter, whereas the majority of flow through the filter is occurring when the filter is saturated. While it is important to assess the travel time of a particle through the filter, the time measured from the first drip test will be longer than the filter's shortest travel time, which will occur when the filter is both full and saturated, and is most likely of more interest in terms of the filter's biological removal effectiveness.

The travel time through the filter also depends on both porosity and hydraulic conductivity, as well as the height of water in the filter, and the relationship between porosity and hydraulic conductivity is not known. It is therefore recommended that this test continue to be performed in conjunction with flow rate testing, as the "first drip" test alone depends upon too many unknown variables and does not present a full picture of the filter's various properties.

Lastly, typical flow rate testing at the factory is done by measuring the volume of water produced by the filter in the first hour of saturated flow. This process can be time-consuming and, as discussed above, may be an inaccurate representation of the filter's performance over time. Because the models presented in this thesis have been developed for a specific filter shape, the observed flow rate through a full filter corresponds to a unique hydraulic conductivity and unique relationships between flow rate and height and between flow rate and time.

Therefore, in order to determine the hydraulic conductivity of the filter as well as how it will perform over time, it is only necessary to find the flow rate when the filter is full, which can be done by simply measuring flow through the filter for a given amount of time, which can be shorter than an hour, while maintaining a constant water height. It is important to ensure that the filter is saturated before beginning this test. This "instantaneous" flow rate at a given height can then be used, based on the results of the model developed in this thesis, to paint a more complete picture of the filter properties.

## Appendix A: Calculation of Head Drop in the Flowerpot Filter

The circular surface area of the top of the water inside the flowerpot filter, $\pi r^2$, can be put in terms of height based on Equation 2-11:

$$A = \pi(0.1769z + 7.35)^2 \quad \text{A-1}$$

The volume of a segment of this filter can be obtained by integrating the circular area inside the filter with respect to height over the change in water height. In the case where we have calculated a known volume based on flow rate at a given initial water height, this method can be used to solve for the final height after the time step $\Delta t$ over which that volume was flowing:

$$\int_{h_1}^{h_2} A(z)dz = V \quad \text{A-2}$$

where $h_1$ is the starting height of the water, $h_2$ is the height of the water after the filter has drained for time $\Delta t$, and $V$ is the volume drained over that time, given by Equation A-3.

In the case of the flowerpot filter, the volume $V$ can be calculated without integration, using the formula for the volume of a conical frustum:

$$V = \frac{1}{3}\pi h(R_1^2 + R_1R_2 + R_2^2) \quad \text{A-3}$$

where $R_1$, $R_2$, and $h$ represent the dimensions of the frustum shown in Figure A-1.

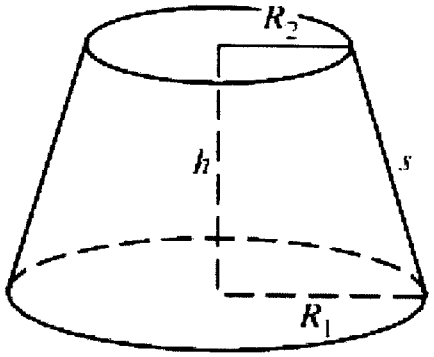


**Figure A-1: Conical frustum (image from Wolfram Alpha)**

The height, $h$, of the frustum, which is equal to the drop in water level $\Delta z$, can be put into terms of the change in radius $\Delta r$ from $R_1$ to $R_2$ by restating Equation 2-11 in terms of $z$:

$$z = 5.65r - 41.5 \quad \text{A-4}$$

and taking the derivative of with respect to $r$:

$$h = \Delta z = 5.65\Delta r \quad \text{A-5}$$

and we can express $\Delta r$ as the difference between the starting and ending radii:

$$\Delta r = R_1 - R_2 \qquad \text{A-6}$$

Equations A-3, A-5, and A-6 can be combined and solved to find the change in radius, $\Delta r$, the subsequent height change, $\Delta h$, and, finally, the new water height in the filter, $h_2$.

## Appendix B: Calculation of Head Drop in the Paraboloid Filter

Miller (2010) gives the following equation for the filter radius $r$ in terms of height $z$ for the paraboloid filter:

$$r = 2.685\sqrt{z} \tag{B-1}$$

We can then find the circular area inside the filter, $\pi r^2$, in terms of height $z$, as:

$$A = \pi(2.685)^2 z \tag{B-2}$$

Integrating this area from the starting height $h_1$ to the new lower water height $h_2$ gives the change in volume $\Delta V$ for the associated head drop:

$$\int_{h_2}^{h_1} \pi(2.685)^2 z \, dz = \Delta V \tag{B-3}$$

We can solve this integral and rearrange to find $h_2$, the new water height after the volume $\Delta V$ has flowed out of the filter:

$$h_2 = \sqrt{h_1^2 - \frac{2\Delta V}{2.685^2 \pi}} \tag{B-4}$$

## Appendix C: Calculation of Head Drop in the Hemispheric Filter

To find the drop in water level for the hemispheric filter, we can take a similar approach to that used for the other two filters. The equation describing the circular cross-section of the inner surface of the hemispheric filter is given by:

$$r^2 + (z - 17.907)^2 = 17.907^2 \qquad \text{C-1}$$

for $r$ and $z$ coordinates given in centimeters. The volume $dV$ of a segment of this hemisphere can be found using the equation:

$$dV = \pi r^2 \, dz \qquad \text{C-2}$$

We can integrate this equation to find the volume $\Delta V$ of a region of the hemisphere between heights $h_1$ and $h_2$, combining Equations C-1 and C-2 to put the integral expression in terms of $z$.

$$\pi \int_{h_2}^{h_1} (35.814z - z^2) \, dz = \Delta V \qquad \text{C-3}$$

Solving this integral, we obtain the following equation:

$$h_2^3 - 17.907h_2^2 = \frac{\Delta V}{\pi} + h_1^3 - 17.907h_1^2 \qquad \text{C-4}$$

which can then be solved to find the new height $h_2$ of the water in the filter.

# Appendix D: Numerical Results

**Table D-1: Flowerpot filter flow rate vs water height, K = 0.234 cm/hr**

| Time [hr] | Water height [cm] | Flow rate [L/hr] |
|---|---|---|
| 0 | 21.2 | 2.133 |
| 0.5 | 18.3 | 1.638 |
| 1 | 15.9 | 1.276 |
| 1.5 | 13.9 | 1.001 |
| 2 | 12.2 | 0.811 |
| 2.5 | 10.7 | 0.659 |
| 3 | 9.4 | 0.543 |
| 3.5 | 8.4 | 0.442 |
| 4 | 7.4 | 0.371 |
| 4.5 | 6.6 | 0.321 |
| 5 | 5.9 | 0.273 |
| 5.5 | 5.3 | 0.236 |
| 6 | 4.7 | 0.203 |
| 6.5 | 4.3 | 0.177 |
| 7 | 3.8 | 0.155 |
| 7.5 | 3.4 | 0.136 |
| 8 | 3.1 | 0.121 |

**Table D-2: Flowerpot filter flow rate vs water height, K = 0.42 cm/hr**

| Time [hr] | Water height [cm] | Flow rate [L/hr] |
|---|---|---|
| 0 | 21.2 | 3.797 |
| 0.25 | 18.6 | 3.008 |
| 0.5 | 16.5 | 2.412 |
| 0.75 | 14.6 | 1.963 |
| 1 | 12.9 | 1.665 |
| 1.25 | 11.5 | 1.317 |
| 1.5 | 10.3 | 1.101 |
| 1.75 | 9.2 | 0.927 |
| 2 | 8.3 | 0.794 |
| 2.25 | 7.4 | 0.674 |
| 2.5 | 6.7 | 0.581 |
| 2.75 | 6.1 | 0.504 |
| 3 | 5.5 | 0.440 |
| 3.25 | 5.0 | 0.387 |
| 3.5 | 4.5 | 0.339 |
| 3.75 | 4.1 | 0.301 |
| 4 | 3.8 | 0.270 |
| 4.25 | 3.4 | 0.240 |
| 4.5 | 3.1 | 0.216 |
| 4.75 | 2.8 | 0.192 |

**Table D-3: Flowerpot filter flow rate vs water height, K = 0.83 cm/hr**

| Time [hr] | Water height [cm] | Flow rate [L/hr] |
|---|---|---|
| 0 | 21.2 | 7.595 |
| 0.2 | 17.0 | 5.109 |
| 0.4 | 13.8 | 3.569 |
| 0.6 | 11.3 | 2.568 |
| 0.8 | 9.4 | 1.921 |
| 1 | 7.8 | 1.705 |
| 1.2 | 6.4 | 1.088 |
| 1.4 | 5.4 | 0.861 |
| 1.6 | 4.6 | 0.697 |
| 1.8 | 3.9 | 0.566 |
| 2 | 3.3 | 0.463 |
| 2.2 | 2.9 | 0.395 |
| 2.4 | 2.5 | 0.334 |
| 2.6 | 2.1 | 0.286 |
| 2.8 | 1.8 | 0.248 |

**Table D-4: Paraboloid filter flow rate vs water height, K = 0.234 cm/hr**

| Time [hr] | Water height [cm] | Flow rate [L/hr] |
|---|---|---|
| 0 | 21.2 | 1.761 |
| 1 | 17.1 | 1.034 |
| 2 | 14.2 | 0.685 |
| 3 | 11.9 | 0.466 |
| 4 | 10.0 | 0.326 |
| 5 | 8.5 | 0.231 |
| 6 | 7.2 | 0.164 |
| 7 | 6.1 | 0.120 |
| 8 | 5.1 | 0.085 |
| 9 | 4.4 | 0.062 |
| 10 | 3.7 | 0.045 |
| 11 | 2.6 | 0.032 |
| 12 | 2.1 | 0.027 |

**Table D-5: Paraboloid filter flow rate vs water height, K = 0.42 cm/hr**

| Time [hr] | Water height [cm] | Flow rate [L/hr] |
|---|---|---|
| 0 | 21.2 | 2.950 |
| 0.5 | 17.9 | 2.004 |
| 1 | 15.2 | 1.404 |
| 1.5 | 13.0 | 0.998 |
| 2 | 11.2 | 0.720 |
| 2.5 | 9.6 | 0.530 |
| 3 | 8.3 | 0.394 |
| 3.5 | 7.2 | 0.292 |
| 4.5 | 5.1 | 0.149 |
| 5.5 | 3.6 | 0.075 |
| 6.5 | 2.5 | 0.039 |

**Table D-6: Paraboloid filter flow rate vs water height, K = 0.83 cm/hr**

| Time [hr] | Water height [cm] | Flow rate [L/hr] |
|---|---|---|
| 0 | 21.2 | 5.924 |
| 0.25 | 17.9 | 4.028 |
| 0.5 | 15.2 | 2.800 |
| 0.75 | 13.0 | 1.988 |
| 1 | 11.1 | 1.440 |
| 1.25 | 9.6 | 1.060 |
| 1.5 | 8.3 | 0.788 |
| 1.75 | 7.2 | 0.584 |
| 2.25 | 5.1 | 0.296 |
| 2.75 | 3.5 | 0.150 |
| 3.25 | 2.5 | 0.076 |

**Table D-7: Hemispheric filter flow rate vs water height, K = 0.234 cm/hr**

| Time [hr] | Water height [cm] | Flow rate [L/hr] |
|---|---|---|
| 0 | 19 | 2.584 |
| 0.5 | 17.7 | 2.258 |
| 1 | 16.6 | 1.971 |
| 1.5 | 15.6 | 1.767 |
| 2 | 14.7 | 1.550 |
| 2.5 | 13.9 | 1.386 |
| 3 | 13.1 | 1.245 |
| 3.5 | 12.5 | 1.118 |
| 4 | 11.8 | 1.009 |
| 4.5 | 11.3 | 0.915 |
| 5 | 10.7 | 0.831 |
| 5.5 | 10.2 | 0.757 |
| 6 | 9.8 | 0.691 |
| 6.5 | 9.3 | 0.630 |
| 7 | 8.9 | 0.580 |
| 7.5 | 8.5 | 0.527 |
| 8 | 8.2 | 0.483 |
| 9 | 7.5 | 0.404 |
| 10 | 6.8 | 0.339 |
| 11 | 6.3 | 0.287 |
| 12 | 5.8 | 0.242 |
| 13 | 5.3 | 0.206 |
| 14 | 4.9 | 0.176 |
| 15 | 4.5 | 0.148 |
| 16 | 4.1 | 0.127 |
| 17 | 3.8 | 0.108 |
| 18 | 3.5 | 0.093 |
| 19 | 3.3 | 0.081 |
| 20 | 3.0 | 0.068 |
| 21 | 2.8 | 0.059 |

**Table D-8: Hemispheric filter flow rate vs water height, K = 0.42 cm/hr**

| Time [hr] | Water height [cm] | Flow rate [L/hr] |
|---|---|---|
| 0 | 19 | 4.601 |
| 0.25 | 17.9 | 4.076 |
| 0.5 | 16.9 | 3.633 |
| 0.75 | 15.9 | 3.254 |
| 1 | 15.1 | 2.930 |
| 1.25 | 14.4 | 2.649 |
| 1.5 | 13.7 | 2.402 |
| 1.75 | 13.0 | 2.184 |
| 2 | 12.5 | 1.990 |
| 2.25 | 11.9 | 1.818 |
| 2.5 | 11.4 | 1.666 |
| 2.75 | 10.9 | 1.527 |
| 3 | 10.5 | 1.405 |
| 3.25 | 10.0 | 1.294 |
| 3.5 | 9.6 | 1.950 |
| 3.75 | 9.2 | 1.105 |
| 4 | 8.9 | 1.019 |
| 4.5 | 8.2 | 0.866 |
| 5 | 7.6 | 0.738 |
| 5.5 | 7.0 | 0.632 |
| 6 | 6.5 | 0.545 |
| 6.5 | 6.0 | 0.469 |
| 7 | 5.6 | 0.408 |
| 7.5 | 5.2 | 0.351 |
| 8 | 4.8 | 0.305 |
| 8.5 | 4.5 | 0.263 |
| 9 | 4.2 | 0.228 |
| 9.5 | 3.9 | 0.203 |
| 10 | 3.6 | 0.174 |
| 10.5 | 3.2 | 0.136 |
| 11 | 3.0 | 0.117 |
| 11.5 | 2.75 | 0.103 |

**Table D-9: Hemispheric filter flow rate vs water height, K = 0.83 cm/hr**

| Time [hr] | Water height [cm] | Flow rate [L/hr] |
|---|---|---|
| 0 | 19.0 | 9.201 |
| 0.15 | 17.6 | 7.947 |
| 0.3 | 16.4 | 6.919 |
| 0.45 | 15.4 | 6.078 |
| 0.6 | 14.5 | 5.271 |
| 0.75 | 13.6 | 4.768 |
| 0.9 | 12.9 | 4.255 |
| 1.05 | 12.2 | 3.803 |
| 1.2 | 11.5 | 3.416 |
| 1.35 | 10.9 | 3.076 |
| 1.5 | 10.4 | 2.779 |
| 1.65 | 9.9 | 2.519 |
| 1.8 | 9.4 | 2.281 |
| 1.95 | 9.0 | 2.069 |
| 2.1 | 8.5 | 1.882 |
| 2.25 | 8.1 | 1.715 |
| 2.4 | 7.8 | 1.534 |
| 2.7 | 7.1 | 1.295 |
| 3 | 6.4 | 1.082 |
| 3.3 | 5.9 | 0.898 |
| 3.6 | 5.4 | 0.752 |
| 3.9 | 4.9 | 0.632 |
| 4.2 | 4.5 | 0.537 |
| 4.5 | 4.1 | 0.446 |
| 4.8 | 3.8 | 0.378 |
| 5.1 | 3.5 | 0.320 |
| 5.4 | 3.2 | 0.274 |
| 5.7 | 2.9 | 0.230 |
| 6 | 2.7 | 0.201 |
| 6.3 | 2.5 | 0.169 |
| 6.6 | 2.2 | 0.141 |
| 6.9 | 2.1 | 0.118 |

## References

Bloem, S.C., van Halem, D., Sampson, M.L., Huoy, L.S. and Heijman, B. (2009). Silver impregnated ceramic pot filter: flow rate versus the removal efficiency of pathogens. *International Ceramic Pot Filter Workshop.* Atlanta, Georgia.

Boschi-Pinto C, Velebit L, and Shibuya K. (2008). Estimating child mortality due to diarrhoea in developing countries. *Bulletin of the World Health Organization.* 86(9):710–717.

Brown, J., Proum, S. and Sobsey, M. (2009) Sustained use of a household-scale water filtration device in rural Cambodia. *Journal of Water and Health* 7(3), 404.

Casanova L., Walters A., Nagahawatte A. and Sobsey M.D. (2012) A post-implementation evaluation of ceramic water purifiers distributed to tsunami-affected communities in Sri Lanka. *Journal of Water and Health* 10(2), 209–220.

Casanova, L, Walters A., Nagahawatte A, and Sobsey MD. (2013). Ceramic water purifier user satisfaction and water quantity production in tsunami-affected Sri Lankan communities. *Journal of Water, Sanitation and Hygiene for Development.* Published online March 7, 2013.

CMWG (2011). Best Practice Recommendations for Local Manufacturing of Ceramic Pot Filters for Household Water Treatment, Ed. 1. The Ceramics Manufacturing Working Group, Centers for Disease Control, Atlanta, Georgia.

DHI-WASY (2012). FEFLOW 6.1 Finite Element Subsurface Flow & Transportation Simulation System User Manual. DHI-WASY GmbH, Berlin, Germany. http://www.feflow.info/uploads/media/users_manual.pdf . Accessed 5/12/13.

Gensburger, I. (2011). Investigation of the critical parameters in the production of ceramic water filters. Technicshe Universiteit Delft, Delft, The Netherlands. October 2011. http://potterswithoutborders.com/wp-content/uploads/2012/07/Delft_Critical-Parameters-in-CWF-Production_Gensburger_RDIC_2011.pdf

Golden Software (2002). Surfer User's Guide; Contouring and 3D Surface Mapping for Scientists and Engineers. Golden Software, Inc., Golden, Colorado. February 2002.

Lantagne, D. (2001). Investigation of the Potters for Peace colloidal silver impregnated ceramic filter report 1: intrinsic effectiveness. Alethia Environmental, Allston, Massachusetts.

Lantagne, D., Klarman, M., Mayer, A., Preston, K., Napotnik, J. and Jellison, K. (2010). Effect of production variables on microbiological removal in locally produced ceramic

filters for household water treatment, *International Journal of Environmental Health Research*, 20(3), 171-187

Lu, C., Miller, M., and Questad, A. (2012). Ghana 2012 Group Project Report. Unpublished Report, Department of Civil and Environmental Engineering, Massachusetts Institute of Technology, Cambridge, Massachusetts.

Miller, T.R. (2010). Optimizing performance of ceramic pot filters in Northern Ghana and modeling flow through paraboloid-shaped filters. Master of Engineering Thesis, Department of Civil and Environmental Engineering, Massachusetts Institute of Technology, Cambridge, Massachusetts.

Miller, M. (2012). Hemispheric Ceramic Pot Filter Evaluation and Quality Assurance Program in Northern Ghana. Master of Engineering Thesis, Department of Civil and Environmental Engineering, Massachusetts Institute of Technology, Cambridge, Massachusetts.

Watters, T. (2010). The Effect of Compositional and Geometrical Changes to the Bending Strength of the Ghanaian Ceramic Pot Filter. Master of Engineering Thesis, Department of Civil and Environmental Engineering, Massachusetts Institute of Technology, Cambridge, Massachusetts.

WHO (2011a). Improved drinking-water source definition. World Health Organization, Geneva, Switzerland. http://www.who.int/healthinfo/statistics/indwatsan/en/index.html. Accessed 12/20/2012.

WHO (2011b). *Guidelines for drinking-water quality, fourth edition.* World Health Organization, Geneva, Switzerland.

WHO (2012). *World health statistics*. World Health Organization, Geneva, Switzerland. http://apps.who.int/iris/bitstream/10665/44844/1/9789241564441_eng.pdf. Accessed 5/12/13.

WHO/UNICEF (2010). *Progress on sanitation and drinking-water: 2010 update.* WHO/UNICEF Joint Monitoring Programme for Water Supply and Sanitation, UNICEF, New York.

WHO/UNICEF (2012). *Progress on drinking water and sanitation: 2012 update.* WHO/UNICEF Joint Monitoring Programme for Water Supply and Sanitation, UNICEF, New York.